LAWRENCE
LIVERMORE
NATIONAL
LABORATORY

UCRL-CONF-216910

Long Term Corrosion Potential and Corrosion Rate of Creviced Alloy 22 in Chloride Plus Nitrate Brines

K. J. Evans, M. L. Stuart, R. A. Etien, G. A. Hust, J. C. Estill, R. B. Rebak

November 8, 2005

Corrosion/2006 Conference and Exposition
San Diego, CA, United States
March 12, 2006 through March 16, 2006

Paper 06623 prepared for Corrosion/2006 Conference and Exposition organized by NACE International (The Corrosion Society) in San Diego, CA 16-21 March 2006

LONG TERM CORROSION POTENTIAL AND CORROSION RATE OF CREVICED ALLOY 22 IN CHLORIDE PLUS NITRATE BRINES

Kenneth J. Evans, Marshall L. Stuart, Robert A. Etien, Gary A. Hust, John C. Estill and Raúl B. Rebak
Lawrence Livermore National Laboratory, Livermore, CA, 94550

ABSTRACT

Alloy 22 is a nickel base alloy highly resistant to all forms of corrosion. In conditions where tight crevices exist in hot chloride containing solutions and at anodic potentials, Alloy 22 may suffer crevice corrosion, a form of localized attack. The occurrence (or not) of crevice corrosion in a given environment (e.g. salt concentration and temperature), is governed by the values of the critical potential (E_{crit}) for crevice corrosion and the corrosion potential (E_{corr}) that the alloy may establish in the studied environment. If E_{corr} is equal or higher than E_{crit}, crevice corrosion may be expected. In addition, it is generally accepted that as Alloy 22 becomes passive in a certain environment, its E_{corr} increases and its corrosion rate (CR) decreases. This paper discusses the evolution of E_{corr} and corrosion rate (CR) of creviced Alloy 22 specimens in six different mixtures of sodium chloride (NaCl) and potassium nitrate (KNO_3) at 100°C. The effect of immersion time on the value of E_{crit} was also determined. Two types of specimens were used, polished as-welded (ASW) and as-welded plus solution heat-treated (ASW+SHT). The latter contained the black annealing oxide film on the surface. Results show that, as the immersion time increases, E_{corr} increased and the CR decreased. Even for highly concentrated brine solutions at 100°C the CR was < 30 nm/year after more than 250 days immersion. Some of the exposed specimens (mainly the SHT specimens) suffered crevice corrosion at the open circuit potential in the naturally aerated brines. Immersion times of over 250 days did not reduce the resistance of Alloy 22 to localized corrosion.

Keywords: N06022, corrosion potential, corrosion rate, chloride, nitrate

INTRODUCTION

Alloy 22 (N06022) is a nickel (Ni) based alloy that contains nominally 22% chromium (Cr), 13% molybdenum (Mo), 3% tungsten (W) and 3% iron (Fe) (ASTM B 575). [1] By virtue of its high level of Cr, Alloy 22 remains passive in most industrial environments and therefore has an exceptionally low general corrosion rate. [2-4] The combined presence of Cr, Mo and W imparts Alloy 22 with high resis-

tance to localized corrosion such as pitting corrosion and stress corrosion cracking even in hot high chloride (Cl^-) solutions. [5-10] It has been reported that Alloy 22 may suffer crevice corrosion when it is anodically polarized in chloride containing solutions. [6-8,11-13] It is also known that the presence of nitrate (NO_3^-) and other oxyanions in the solution minimizes or eliminates the susceptibility of Alloy 22 to crevice corrosion. [6-8,14-20] The value of the ratio ($[Cl^-]/[NO_3^-]$) has a strong effect of the susceptibility of Alloy 22 to crevice corrosion. [14-20] The higher the nitrate to chloride ratio the stronger the inhibition by nitrate.

From the general and localized corrosion point of view, it is important to know the value of E_{corr} for Alloy 22 under different environmental conditions. [16] The corrosion degradation model for the Yucca Mountain nuclear waste container assumes that localized corrosion will only occur when E_{corr} is equal or greater than a critical potential (E_{crit}). [16] That is, if $E_{corr} < E_{crit}$ or $\Delta E = E_{crit} - E_{corr} > 0$, general or passive corrosion will occur and localized corrosion is not expected. Passive corrosion rates of Alloy 22 are generally exceptionally low. In environments that promote localized corrosion, E_{crit} is the lowest potential that would initiate crevice corrosion. The value of E_{crit} is generally ascribed as the repassivation potential for crevice corrosion obtained using the cyclic potentiodynamic polarization (CPP) curve described in ASTM G 61. [16] From the CPP, the repassivation potential is taken as the potential at which the reverse scan line crosses over the forward scan. This potential is called the repassivation potential cross over (ERCO). In short, by knowing the values of E_{corr} and E_{crit} (ERCO) of Alloy 22, the likelihood or necessary conditions for the alloy to suffer crevice corrosion under natural polarization (e.g. oxygen from air) can be established.

Dunn et al. reported that the values of E_{corr} of Alloy 22 in air saturated 4 M Cl^- solution at 95°C were in the range between –300 and –100 mV SCE (-260 to –60 mV SSC). [12] Similarly, the E_{corr} of Alloy 22 in 0.028 M Cl^- pH ~ 10 at 95°C was reported to be between –200 and 0 mV SCE (-160 to +40 mV SSC). [12] Dunn et al. also stated that low temperature air oxidized specimens produced more scattered values of E_{corr} than did polished specimens. [12] In pH 2.7 solution of 0.028 M NaCl at 95°C the stabilized E_{corr} was approximately +250 mV SCE (+290 mV SSC). [12] That is, a lower pH promoted a stronger passivation thus resulting in a higher value of E_{corr}. Similar findings were reported by Estill et al. who reported that in acidic multi-ionic solutions simulating concentrated ground water the E_{corr} of Alloy 22 could be as high as +400 mV SSC at 90°C. [21] However, in pH 10 multi-ionic solutions the steady state E_{corr} was below +100 mV SSC. [21] The increase in the value of E_{corr} is generally accompanied by a decrease in the value of corrosion rate. For example, it was reported that when Alloy 22 was immersed in an acidic aerated multi-ionic solution at 90°C, the E_{corr} increased from approximately –300 mV to +300 mV SSC in one week. [7] At the same time, the corrosion rate dropped one order of magnitude, from approximately 1 μm/year after immersion to approximately 0.1 μm/year after the one-week exposure. [7]

The purpose of the current work was to monitor the behavior of E_{corr} and corrosion rate for welded Alloy 22 creviced specimens in six naturally aerated brines containing varying amounts of chloride and nitrate for over 8 months. The specimens were tested both in the as-welded (ASW) condition and also in the as-welded plus solution heat-treated condition (ASW+SHT). The latter specimens contained the black annealing oxide film on the surface. Preliminary analysis of the data has been published before. [22] The effect of the immersion time on the anodic behavior of Alloy 22 was also determined.

EXPERIMENTAL TECHNIQUE

Alloy 22 (N06022) specimens used to assess corrosion potential (E_{corr}) and corrosion rate (CR) as a function of immersion time were machined from welded 1.25-inch thick plates (~32 mm). Table 1 shows the chemical composition of the heats for the base plate and the welding wire. The plates were

welded using the gas tungsten arc welding (GTAW) technique from both sides of the plate using the double V groove technique. The specimens were in the form of prism crevice assemblies (PCA) (Figure 1). The dimensions of the PCA were: 0.375 inch thick, 0.75 inch high and 0.75 inch wide. The exposed surface area of each specimen was 14.06 cm². This surface area did not include the area covered by the crevice formers, which was approximately 1.5 cm² on each side. The PCA had a mounting mechanism for the connecting rod explained in ASTM G 5 (Figure 1). [23] All the specimens had a weld seam through the center of the cross section. The crevice formers were mounted on both sides of the specimen (Figure 1). Each crevice former consisted of a washer made of a ceramic material containing 12 crevicing spots or teeth with gaps in between the teeth (ASTM G 48). [23] The width of the weld seam was not the same for both faces where the crevice formers (CF) were mounted, that is, in some instances the teeth of the CF were resting solely on weld material and in others on a weld and wrought mix of material. Before mounting them onto the metallic specimens, the CF were covered with PTFE tape to ensure a tight crevicing gap. The specimens had a ground surface finish of 600grit paper. There are two types of specimens in this work: (1) The as-welded (ASW) which were as-received welded specimens and (2) the as-welded plus solution heat treated (ASW + SHT) which were annealed in air for 20 min at 1121°C and then water quenched. The latter specimens were finished with 600-grit paper before the heat treatment but the final oxide formed as a consequence of annealing and water quenching was not disturbed prior to testing. The ASW + SHT specimens were black with slight tones of green, typical of high temperature formed chromium oxide. All the test specimens were fully immersed in the test solution. For each surface and metallurgical condition (ASW and ASW + SHT) there were four PCA specimens of Alloy 22 in each cell or in each electrolyte. The E_{corr} of all eight Alloy 22 specimens were monitored continuously.

In all the environments, the E_{corr} of pure platinum rods (ASTM B 561) [1] was also monitored. The platinum rods were 1/8-inch in diameter and 12-inch long. The rods were immersed 1-inch deep into the electrolyte solutions.

Table 2 shows the composition of the six test solutions expressed in molality (*m*), which represents moles of the salt per kilogram of the solvent (water). The solutions were prepared using sodium chloride (NaCl), potassium nitrate (KNO_3) and de-ionized water. The volume of the electrolyte solution in each cell was 2 liters (2 L). The testing temperature was 100°C. The electrolyte solutions were naturally aerated; that is, the solutions were not purged, but a stream of air was circulated above the level of the solution. This stream of air exited the vessel through a condenser to avoid evaporation of the electrolyte.

The E_{corr} was monitored using saturated silver chloride electrodes [SSC] through a Luggin capillary. The reference electrode was kept at room temperature using a jacketed electrode holder through which cooled water was re-circulated. The potentials in this paper are reported in the saturated silver chloride scale [SSC]. At ambient temperature, the SSC scale is 199 mV more positive than the normal hydrogen electrode (NHE).

The value of the free corrosion potentials or open circuit potentials were acquired using a commercial data acquisition (DA) unit that had the input resistance set at 10 G-ohm. Typically, the measurements were acquired every minute for the first day and every hour after the first day. The data was logged into in the internal memory of the DA unit and simultaneously to a spreadsheet in an interfaced personal computer. Usually, data back up was performed monthly.

At the same time that E_{corr} was being monitored for all eight Alloy 22 specimens, the polarization resistance (PR) of two specimens was also monitored as a function of time using the ASTM G 59 technique. [23] Polarization resistance measurement was performed in one ASW and one ASW + SHT specimen in each cell (marked as PR in Table 3). The resistance to polarization was generally measured at 24 h of the first immersion, at 7 days, at 28 days and at every four weeks after that. The polarization resistance values (Ω.cm²) were later converted to corrosion rates (μm/year). To measure the polarization

resistance, an initial potential of 20 mV below the corrosion potential (E_{corr}) was ramped to a final potential of 20 mV above E_{corr} at a rate of 0.167 mV/s. Linear fits were constrained to the potential range of 10 mV below E_{corr} to 10 mV above E_{corr}. In plot potential vs. current the slope is defined as R_p or resistance to polarization (ASTM G 59). To calculate R_p, the potential was plotted in the X-axis and the current (dependent variable) in the Y-axis. The Tafel constants, b_a and b_c, were assumed to be $\pm$ 0.12 V/decade. Corrosion rates were calculated using Equations 1 and 2

$$i_{corr} = \frac{1}{R_p} \times \frac{b_a \cdot b_c}{2.303(b_a + b_c)} \qquad (1)$$

$$CR(\mu m / yr) = k \frac{i_{corr}}{\rho} EW \qquad (2)$$

Where k is a conversion factor (3.27 x 10^6 $\mu m \cdot g \cdot A^{-1} \cdot cm^{-1} \cdot yr^{-1}$), i_{corr} is the corrosion current density in A/cm^2, which is calculated from resistance to polarization (R_p) slopes, EW is the equivalent weight of Alloy 22 (23.28 g), and ρ is the density of Alloy 22 (8.69 g/cm^3). The EW was calculated assuming an equivalent dissolution of the major alloying elements as Ni^{2+}, Cr^{3+}, Mo^{6+}, Fe^{2+}, and W^{6+} (ASTM G 102). [23]

The start and finish date for each cell are given in Table 3. At the finish date, a cyclic potentiodynamic polarization (CPP) was performed on the same specimens that were used for polarization resistance tests (Table 3). Then the specimens were removed from the cells, disassembled and then were examined under 20X magnification for evidence of localized corrosion (mainly crevice corrosion).

EXPERIMENTAL RESULTS AND DISCUSSION

Evolution of the Corrosion Potential of Alloy 22

Table 3 lists the E_{corr} of Alloy 22 and platinum in the six electrolyte solutions (Cells 22 through 27) at one day after the tests started and at a fixed later date towards the end of the immersion test. The immersion tests in Cells 22-27 were terminated on 19Nov04. The exposure time for the specimens in all the cells was always longer than 8 months or 250 days (Table 3).

Figures 2-7 show the evolution of the E_{corr} of platinum and Alloy 22 vs. the immersion time in Cells 22 through 27. Platinum is considered an inert electrode in many environments and therefore the value of E_{corr} of platinum is a measure of the redox potential of the system. For clarity, only the data for one of each Alloy 22 specimen type (ASW and ASW + SHT) is shown. Data plotted in Figures 2-7 were taken at weekly intervals (each Friday at 14:00).

Figures 2-5 show the values of E_{corr} as a function of time in 1 m and 3.5 m NaCl solutions (Cells 26, 27, 24 and 25). The E_{corr} of Pt was stable as a function of time at slightly above 200 mV. The E_{corr} of ASW + SHT Alloy 22 increased rather rapidly in the first few days of immersion and then increased slower or remained stable at approximately 0 mV. The E_{corr} of ASW Alloy 22 slowly increased as the immersion time increased, and at the end of the testing periods the E_{corr} of ASW material did not seem to have reached the steady-state value. The data presented reflect the results for 8+ months of testing. Testing could not continue for longer times due to a laboratory consolidation process in November 2004. Figures 6-7 show similar plots of E_{corr} vs. time in 6 m NaCl solutions (Cells 22 and 23). The behavior of the three electrodes in 6 m NaCl solution is similar than in the lower salt solutions (Figures 2-5), except for the potential of the Pt electrode, which is slightly higher. Figures 2-7 also show that the instant value of E_{corr} for the ASW + SHT specimens was more erratic than that for ASW specimens. It

may be assumed that the fluctuations in the E_{corr} of the ASW + SHT specimens could be associated to nucleation and further repassivation of crevice corrosion. When crevice corrosion is initiated the E_{corr} drops which causes the crevice corrosion to repassivate which in turn causes the E_{corr} to increase again.

In general, for all the cells, the E_{corr} values of the ASW + SHT specimens were higher than those of the ASW specimens. It may be assumed that eventually for further immersion times, the values of E_{corr} of the ASW specimens would have reached the values of the E_{corr} of the ASW + SHT specimens (Figures 2-7).

The Long Term Corrosion Potential of Alloy 22 and Platinum

Figure 8 shows the long-term (>8 months) average E_{corr} of Alloy 22 both for ASW and ASW + SHT specimens as a function of the concentration of nitrate in the electrolyte solutions. Each point is the average of four different values (from Table 3). The standard deviation of the values is shown as error bars. The standard deviation of the E_{corr} for the ASW + SHT specimens is higher than for the ASW specimens; that is, the values of E_{corr} for specimens with a freshly-ground surface were more reproducible than for the specimens containing a high temperature formed oxide scale on the surface. Figure 8 also shows that the average E_{corr} of ASW specimens (freshly ground surface) was approximately 100 mV lower than the E_{corr} of ASW + SHT specimens (with black annealed oxide film). It is possible that the E_{corr} for ASW specimen has not yet reached steady state even after the 8+ months of immersion (Figures 2-7). In addition, Figure 8 shows that E_{corr} of Alloy 22 does not depend strongly on the total amount of nitrate present in these solutions. Furthermore, Figure 8 shows that the E_{corr} of platinum was higher than the E_{corr} for Alloy 22 and independent of the concentration of nitrate.

Figure 9 shows the long-term average E_{corr} of Alloy 22 as a function of total chloride concentration in the cells. Each point represents the average of four individual values (from Table 3). Error bars are not shown for clarity. For each chloride concentration, E_{corr} was higher for the ASW + SHT specimens than for the ASW specimens. Average values of E_{corr} or both Alloy 22 types of specimens for each chloride concentration were highly reproducible, especially considering that, for example, each of the average values of E_{corr} at each chloride concentration corresponded to different concentration values of nitrate. E_{corr} values in Figure 9 seem to suggest that the E_{corr} of Alloy 22 is not a linear function of chloride concentration.

Figure 10 shows the long-term average E_{corr} of Alloy 22 as a function of the ratio of nitrate to chloride. Each point represents the average of four individual values (from Table 3). E_{corr} was approximately 100 mV higher for the ASW + SHT specimens than for the ASW specimens. Error bars are not shown for clarity. Data in Figure 10 show that the E_{corr} of Alloy 22 is not highly dependent on the nitrate over chloride concentration for the two values shown.

The Corrosion Rate of Alloy 22

Figures 11-16 show the corrosion rate of Alloy 22 specimens as a function of immersion time at 100°C for the six studied cells (22 though 27). In general, as the immersion time increased the corrosion rate for both type of specimens decreased. In general, for the couple of months of immersion, the corrosion rate of the ASW + SHT specimens was higher than for the ASW specimens. However, for longer immersion times, the corrosion rate for both types of specimens was equivalent and the trend appeared to reverse (Figures 14 and 15). The final measured corrosion rate for both types of specimens was in general on the order of 0.02 to 0.03 μm/year or 20 to 30 nm/year (Figure 17). This is a remarkable low value of corrosion rate considering the concentration and temperature of the testing brines. In general, for the less concentrated solution (Figure 12) the results of corrosion rate seem less reproducible than for the more concentrated solution (Figure 15).

Table 4 shows the average long-term (for duration longer than 250 days) corrosion rates for all the specimens tested in Cells 22-27 as well as the standard deviations of the corrosion rate values. Table 4 shows that the average corrosion rate (for all the cells) of ASW specimens was lower (0.026 μm/year) than the average corrosion rate of the ASW + SHT specimens (0.033 μm/year). Table 4 also shows that the standard deviation of the corrosion rate for the ASW + SHT specimens was approximately twice as much as for the ASW specimens. Figures 17 and 18 show the long-term corrosion rates (from Table 4) for both types of Alloy 22 specimens (ASW and ASW + SHT) as a function of the amount of nitrate and chloride in the solutions, respectively. For clarity, the error bars of the standard deviation are not shown but their values are given in Table 4. Except for two values, the corrosion rates of the ten other specimens seem to fall in the order of 20 to 30 nm/year. In the studied conditions, the amount of nitrate or chloride in the solution did not seem to impact the value of the corrosion rate (Figures 17 and 18). The two values of corrosion rate that are slightly higher could correspond to specimens that were undergoing crevice corrosion when the polarization resistance tests were conducted.

Effect of Immersion time on the Anodic Polarization of Alloy 22

Figures 19-24 show the cyclic potentiodynamic polarization (CPP) curves for Alloy 22 creviced specimens in electrolyte solutions containing from 1 m NaCl to 6 m NaCl (Table 2). Each figure contains three CPP curves, one for a freshly exposed specimen in deaerated solutions, one for a polished specimen after more than 8 months in the Cells (Table 2) and one for the SHT also after 8 months exposure. The characteristic values of potential for these tests are listed in Table 5 (for the >8 months in the aerated Cells) and in Table 6 for the freshly polished specimens in the deaerated electrolytes. In Tables 5-6 the E_{corr} is the value of the open circuit potential just before performing the CPP test, E20 and E200 represent values of breakdown potential and are the values of potential for which the current density in the forward scans reach 20 and 200 μA/cm², respectively. ER1 and ER10 represent values of repassivation potential and are the values of potential for which the current density in the reverse scans reach 10 and 1 μA/cm², respectively. ERCO is the repassivation potential cross-over, which is the potential at which the reverse scan intercepts the forward scan.

The effect of the black annealing oxide film (BOF) for the SHT specimens tested only after 24-h exposure to the electrolyte is given in a companion paper 06624. [24]

Figures 19-24 show consistent findings regarding the effect of immersion time on the anodic behavior of Alloy 22. The corrosion potential of the >8 months immersed specimens in aerated solutions was in general approximately 400 mV higher than the corrosion potential of the freshly polished specimens immersed in deaerated electrolytes for 24-h. Also, the anodic current density of the >8 months immersed specimens was in general on the order of one to two orders of magnitude lower than for the 24-h immersed specimens. In most of the tests, the breakdown potential for the >8 months immersed specimens was higher than for the 24-h immersed specimens. All the observations from Figures 19-24 show that the specimens immersed for long time in the electrolyte solutions did not become more susceptible to corrosion. That is, the use of short-term data for corrosion behavior evaluation seems to be conservative.

Typical Potentials from the Cyclic Potentiodynamic Polarization Curves

Figure 25 shows the breakdown potential (E20) for Alloy 22 in a 6 m NaCl solution containing both 0.3 m and 0.9 m KNO_3 at 100°C. The data for the freshly exposed specimens are plotted as average values with the error bar representing the standard deviation (data from Table 6). For the >8 months immersion the symbols represent single values (Table 5). Figure 25 shows that the breakdown potential increased approximately 300 mV for the specimens exposed longer time in the electrolyte solution. Fig-

ure 26 is a similar representation for the repassivation potential (ER1). Similarly as for E20 (Figure 25), ER1 increased as the exposure time increased (Figure 26). The increase in ER1 seems to be higher for the higher nitrate to chloride ratio solution. It is likely that the longer immersion times allowed for Alloy 22 to develop an oxide film more resistant to breakdown and easier to repair after breakdown is forced by the anodic polarization. The development of a more resistant oxide film for longer immersion times is explained by the annihilation of defects in the oxide as the time increases. [25]

Figure 27 shows the >8 months values of E_{corr} for ASW and ASW + SHT specimens as a function of the nitrate concentration (similar to Figure 8). Figure 8 also shows the average values of ERCO for freshly polished specimens from Table 6. It has been hypothesized earlier that whenever E_{corr} is higher than ERCO, crevice corrosion could be expected. This hypothesis is a necessary but not a sufficient condition for crevice corrosion to occur. Figure 27 suggests that the ASW + SHT specimens could be more sensitive to crevice corrosion since their E_{corr} values are higher than the ERCO values measured using CPP curves (Table 6).

Observation of Creviced Specimens After >8 Months in Aerated Electrolytes

Table 7 shows the characteristics of the specimens that were examined after more than 8 months exposure at the open circuit potential to naturally aerated electrolytes at 100°C. These specimens are listed in Table 3 and there are three specimens studied for each Cell and each surface condition (ASW vs. ASW + SHT). The fourth specimen was polarized during the CPP as identified in Table 3 and Figures 19-24. Table 7 shows that the ASW + SHT specimens were more prone to crevice corrosion than the ASW specimens. However, the amount of crevice corrosion attack was small. For the same chloride concentration, the specimens exposed to the higher nitrate to chloride ratio suffered less crevice corrosion than the specimens with lower nitrate to chloride ratio (Table 7). The most aggressive solutions seemed to be 1 m NaCl and 6 m NaCl. Fewer cases of crevice corrosion attack were found in the 3.5 m NaCl solutions.

The results in Table 7 confirm the predictions of Figure 27, that is, the ASW + SHT specimens seem less resistant to crevice corrosion than the ASW specimens. However, the results in Table 7 show that the attack was not as extensive in the specimens as it may be predicted by the data in Figure 27. This could be because the repassivation potential for the longer immersed specimens seemed to increase (Figure 26) for the longer immersion times.

Concluding Remarks

All the ASW specimens always showed a steady increase in the E_{corr} as the time increased (Figures 2-7). However the ASW + SHT specimens sometimes showed fluctuations in the E_{corr} value of 200 mV (Figures 2-7) that could be attributed to the occurrence of crevice corrosion. This has been confirmed by observation of the specimens after >8 months exposure. It has been reported before that specimens with air formed oxide films may yield less predictable E_{corr}. [12] The fluctuations in the E_{corr} values for ASW + SHT specimens did not seem to be reflected in the values of corrosion rate, which sometimes also fluctuated more than the corrosion rate values for ASW specimens (Figures 11-16). During the fluctuations, as E_{corr} decreases, the corrosion rate increases. These fluctuations in the corrosion rates are also reflected in the higher values of standard deviation for the ASW + SHT specimens (Table 4).

Figure 8 shows that the average E_{corr} of Alloy 22 (and even Pt) does not seem to increase as the amount of nitrate in the solution increased. This finding was unexpected. Figure 17 also shows that the average corrosion rate does not depend strongly on the amount of nitrate in the solution.

In general, the corrosion rate data calculated using the polarization resistance technique (ASTM G 59) showed that the values were extremely small, in the order of 30 nm/year or less (Figure 17 and Table 4). The tested conditions in this work were highly aggressive, since they were aerated brines at 100°C with salt contents of up to 30% by weight. This salt content is approximately ten times higher than the salt content in seawater. In spite of the harsh tested conditions, and considering that the specimens were tightly creviced, the overall corrosion rate of Alloy 22 was negligible. When crevice corrosion occurs E_{corr} would move to a more cathodic (active) potential and the output polarization resistance (R_p) should decrease. The fact that the general corrosion remained so low (or the R_p so high) suggests that all the tested specimens remained mostly in the passive state, that is, when crevice corrosion occurred, it was minimal and short-lived.

The effect of immersion time on the resistance of Alloy 22 to localized corrosion was always a matter of debate. Most of the data for the critical potential or repassivation potential for Alloy 22 was obtained only after immersing the Alloy 22 specimens for 24 h in deaerated electrolytes. [16] This is a standard testing procedure (e.g. ASTM G 61). Therefore, it was of interest to determine if longer immersion times could affect the value of repassivation potential. Figure 26 shows that the repassivation potential only increases after an 8+ month immersion in the concentrated brines. That is, the values used for the model of localized corrosion used conservative lower values. [16]

Localized corrosion such as crevice corrosion only occurs above a critical potential. If the applied potential to the specimen in the environment of interest is below this critical potential, crevice corrosion will not occur. This critical potential for crevice corrosion is generally associated with the crevice repassivation potential. [16] Figure 27 shows the average E_{corr} in the aerated brine solutions for ASW PCA specimens. Table 6 also shows the repassivation potential (ERCO) for ASW creviced multiple crevice assembly (MCA) or lollipop specimens in the same (deaerated) solutions. [17] Figure 27 shows that for most of the ASW + SHT specimens, E_{corr} was higher than ERCO, suggesting that these specimens could be susceptible to crevice corrosion under the open circuit potentials. The observations in Table 7 of the exposed specimens confirm this finding.

CONCLUSIONS

(1) In the six tested aerated electrolytes, E_{corr} of Alloy 22 increased as a function or the immersion time. For the ASW specimens the increase was more gradual than for the SHT specimens.

(2) The long-term E_{corr} (>250 days) of Alloy 22 was higher for the SHT specimens than for the ASW specimens.

(3) There was little or no effect of total $[NO_3^-]$, total $[Cl^-]$ and $[Cl^-]/[NO_3^-]$ on the E_{corr} of Alloy 22.

(4) The corrosion rate of both ASW and SHT Alloy 22 decreased as the immersion time increased. The largest decrease in corrosion rate occurred in the first 30 days of immersion.

(5) For both ASW and ASW + SHT Alloy 22, the corrosion rate after 250 days of immersion was on the order of 30 nm/year and it did not depend on the composition of the electrolyte.

(6) Both the breakdown and the repassivation potential of specimens immersed for over 8 months in the hot electrolytes increased with respect to the same characteristic potentials for specimens immersed for 24-h in deaerated electrolytes.

(7) Observation of the exposed specimens after 8+ months immersion showed that the ASW + SHT specimens were more susceptible to crevice corrosion under open circuit conditions in aerated brines. However, when crevice corrosion attack occurred, it was minimal.

ACKNOWLEDGMENTS

Sharon G. Torres and her group are acknowledged for performing the solution heat treatments of the specimens. This work was performed under the auspices of the U. S. Department of Energy by the University of California Lawrence Livermore National Laboratory under contract N° W-7405-Eng-48. This work is supported by the Yucca Mountain Project, which is part of the DOE Office of Civilian Radioactive Waste Management (OCRWM)

REFERENCES

1. ASTM International, Volume 02.04, Standard B 575 (ASTM International, 2003: West Conshohocken, PA).
2. Haynes International, “Hastelloy C-22 Alloy”, Brochure H-2019E (Haynes International, 1997: Kokomo, IN).
3. R. B. Rebak in Corrosion and Environmental Degradation, Volume II, p. 69, Wiley-VCH, Weinheim, Germany (2000).
4. R. B. Rebak and P. Crook “Influence of the Environment on the General Corrosion Rate of Alloy 22,” PVP-Vol 483 pp. 131-136 (ASME, 2004: New York, NY).
5. R. B. Rebak and P. Crook “Improved Pitting and Crevice Corrosion Resistance of Nickel and Cobalt Based Alloys,” ECPV 98-17, pp. 289-302 (The Electrochemical Society, 1999: Pennington York, NJ).
6. B. A. Kehler, G. O. Ilevbare and J. R. Scully, Corrosion, 1042 (2001).
7. K. J. Evans and R. B. Rebak in Corrosion Science – A Retrospective and Current Status in Honor of Robert P. Frankenthal, PV 2002-13, p. 344-354 (The Electrochemical Society, 2002: Pennington, NJ).

8. K. J. Evans, S. D. Day, G. O. Ilevbare, M. T. Whalen, K. J. King, G. A. Hust, L. L. Wong, J. C. Estill and R. B. Rebak, PVP-Vol. 467, Transportation, Storage and Disposal of Radioactive Materials – 2003, p. 55 (ASME, 2003: New York, NY).
9. Y-M. Pan, D. S. Dunn and G. A. Cragnolino in Environmentally Assisted Cracking: Predictive Methods for Risk Assessment and Evaluation of Materials, Equipment and Structures, STP 1401, pp. 273-288 (West Conshohocken, PA: ASTM 2000).
10. R. B. Rebak in Environmentally Assisted Cracking: Predictive Methods for Risk Assessment and Evaluation of Materials, Equipment and Structures, STP 1401, pp. 289-300 (West Conshohocken, PA: ASTM 2000).
11. C. S. Brossia, L. Browning, D. S. Dunn, O. C. Moghissi, O. Pensado and L. Yang "Effect of Environment on the Corrosion of Waste Package and Drip Shield Materials," Publication of the Center for Nuclear Waste Regulatory Analyses (CNWRA 2001-03), September 2001.
12. D. S. Dunn, L. Yang, Y.-M. Pan and G. A. Cragnolino "Localized Corrosion Susceptibility of Alloy 22," Paper 03697 (NACE International, 2003: Houston, TX).
13. K. J. Evans, A. Yilmaz, S. D. Day, L. L. Wong, J. C. Estill and R. B. Rebak "Comparison of Electrochemical Methods to Determine Crevice Corrosion Repassivation Potential of Alloy 22 in Chloride Solutions," JOM, January 2005 (to be published).
14. G. A. Cragnolino, D. S. Dunn and Y.-M. Pan "Localized Corrosion Susceptibility of Alloy 22 as a Waste Package Container Material," Scientific Basis for Nuclear Waste Management XXV, Vol. 713 (Materials Research Society 2002: Warrendale, PA).
15. D. S. Dunn and C. S. Brossia "Assessment of Passive and Localized Corrosion Processes for Alloy 22 as a High-Level Nuclear Waste Container Material," Paper 02548 (NACE International, 2002: Houston, TX).
16. J. H. Lee, T. Summers and R. B. Rebak "A Performance Assessment Model for Localized Corrosion Susceptibility of Alloy 22 in Chloride Containing Brines for High Level Nuclear Waste Disposal Container," Paper 04692 (NACE International, 2004: Houston, TX).
17. G. O. Ilevbare, K. J. King, S. R. Gordon, H. A. Elayat, G. E. Gdowski and T. S. E. Summers "Effect of Nitrate on the Repassivation Potential of Alloy 22 in Chloride Containing Solutions," Meeting of the Electrochemical Society, 03-08Oct04, Honolulu, HI p. 285 (The Electrochemical Society, 2005: Pennington, NJ).
18. D. S. Dunn, L. Yang, C. Wu and G. A. Cragnolino, Material Research Society Symposium, Spring 2004, San Francisco, Proc. Vol 824 (MRS, 2004: Warrendale, PA)
19. D. S. Dunn, Y.-M. Pan, K. Chiang, L. Yang, G. A Cragnolino and X. He "Localized Corrosion Resistance and Mechanical Properties of Alloy 22 Waste Package Outer Containers" JOM, January 2005, pp 49-55.
20. R. B. Rebak, Paper 05610, Corrosion/2005 (NACE International, 2005: Houston, TX)
21. J. C. Estill, G. A. Hust and R. B. Rebak "Long Term Corrosion Potential Behavior of Alloy 22," Paper 03688 (NACE International, 2003: Houston, TX).
22. K. J. King, J. C. Estill, G. A. Hust, M. L. Stuart and R. B. Rebak, Paper 05607, Corrosion/2005 (NACE International, 2005: Houston, TX).
23. ASTM International, Volume 03.02, Standards G 5, G 48, G 59, G 61, G 102 (ASTM International, 2003: West Conshohocken, PA).
24. R. B. Rebak, R. A. Etien, S. R. Gordon and G. O. Ilevbare, Paper 06624, Corrosion/2006 (NACE International, 2006: Houston, TX).
25. R. M. Carranza, M. A. Rodríguez and R. B. Rebak, Paper 06-02, 16th International Corrosion Congress, Beijing, China 19-24 September 2005.

TABLE 1
CHEMICAL COMPOSITION OF THE PRISM CREVICE ASSEMBLIES (PCA (Wt%)

Elements ?	Ni	Cr	Mo	W	Fe	Others
Nominal ASTM B 575	50-62	20-22.5	12.5-14.5	2.5-3.5	2-6	2.5Co-0.5Mn-0.35V max
PCA Specimens Heats						
KE0151-0239 Base Heat 2277-0-3183	55.29	21.23	13.37	2.93	3.65	1.7Co-0.23Mn-0.14V
KE0151-0239 Weld Wire Heat XX1829BG	59.31	20.44	14.16	3.07	2.2	0.21Mn-0.15Cu

TABLE 2
COMPOSITION OF THE ELECTYROLYTE SOLUTIONS (m)

Cells / Species	$[Cl^-]$ (m)	$[NO_3^-]$ (m)	$[Cl]/[NO_3^-]$	$[NO_3^-]/[Cl^-]$
23	6	0.9	6.67	0.15
22	6	0.3	20	0.05
24	3.5	0.525	6.67	0.15
25	3.5	0.175	20	0.05
26	1	0.15	6.67	0.15
27	1	0.05	20	0.05

TABLE 3
LIST OF CELL AND SPECIMENS FOR CORROSION POTENTIAL (E_{corr})
AND CORROSION RATE MONITORING

Channel – Type of Test	Specimen Type and Number	E_{corr} (mV, SSC) 1 Day	E_{corr} (mV, SSC) >8 months
CELL 22: 6 m NaCl + 0.3 m KNO_3 pH 6.67, 100°C [Cl^-/NO_3^- = 20, NO_3^-/Cl^- = 0.05] Starting Date: 20Jan04. End Date: 19Nov04, Days in Testing = 304			
		21Jan04	25Oct04
102–PR&CPP	N06022 ASW PCA KE0124	-191	-126
103	N06022 ASW PCA KE0121	-177	-138
104	N06022 ASW PCA KE0122	-182	-120
105	N06022 ASW PCA KE0123	-163	-128
106–PR&CPP	N06022 ASW + SHT PCA KE0189	-43	15
107	N06022 ASW + SHT PCA KE0187	-200	-77
108	N06022 ASW + SHT PCA KE0188	-163	22
109	N06022 ASW + SHT PCA KE0186	-185	12
101	Wrought Platinum Rod WEA019	-185	266
CELL 23: 6 m NaCl + 0.9 m KNO_3 pH 6.3, 100°C [Cl^-/NO_3^- = 6.67, NO_3^-/Cl^- = 0.15] Starting Date: 04Feb04. End Date: 19Nov04, Days in Testing = 289			
		05Feb04	25Oct04
202–PR&CPP	N06022 ASW PCA KE0125	-262	-81
203	N06022 ASW PCA KE0126	-207	-70
204	N06022 ASW PCA KE0127	-207	-78
205	N06022 ASW PCA KE0128	-233	-93
206–PR&CPP	N06022 ASW + SHT PCA KE0190	-328	154
207	N06022 ASW + SHT PCA KE0191	-209	161
208	N06022 ASW + SHT PCA KE0192	-258	204
209	N06022 ASW + SHT PCA KE0193	-202	-48
201	Wrought Platinum Rod WEA027	188	278
CELL 24: 3.5 m NaCl + 0.525 m KNO_3 pH 7.24, 100°C [Cl^-/NO_3^- = 6.67, NO_3^-/Cl^- = 0.15] Starting Date: 23Feb04. End Date: 19Nov04, Days in Testing = 270			
		24Feb04	04Nov04
102–PR&CPP	N06022 ASW PCA KE0129	-172	-150
103	N06022 ASW PCA KE0130	-168	-152
104	N06022 ASW PCA KE0131	-174	-154
105	N06022 ASW PCA KE0132	-178	-152
106–PR&CPP	N06022 ASW + SHT PCA KE0194	-39	-3
107	N06022 ASW + SHT PCA KE0195	-21	-5
108	N06022 ASW + SHT PCA KE0196	-20	-21
109	N06022 ASW + SHT PCA KE0197	-31	-31
101	Wrought Platinum Rod WEA029	174	234

TABLE 3 - CONTINUED

CELL 25: 3.5 m NaCl + 0.175 m KNO_3 pH 7.0, 100°C [Cl^-/NO_3^- = 20, NO_3^-/Cl^- = 0.05]
Starting Date: 27Feb04. End Date: 19Nov04, Days in Testing = 262

		28Feb04	04Nov04
202–PR&CPP	N06022 ASW PCA KE0133	-142	-131
203	N06022 ASW PCA KE0134	-157	-155
204	N06022 ASW PCA KE0135	-153	-136
205	N06022 ASW PCA KE0136	-163	-121
206–PR&CPP	N06022 ASW + SHT PCA KE0198	-58	8
207	N06022 ASW + SHT PCA KE0199	-75	-68
208	N06022 ASW + SHT PCA KE0200	-29	54
209	N06022 ASW + SHT PCA KE0201	-47	-5
201	Wrought Platinum Rod WEA017	217	229

CELL 26: 1 m NaCl + 0.15 m KNO_3 pH 7.61, 100°C [Cl^-/NO_3^- = 6.67, NO_3^-/Cl^- = 0.15]
Starting Date: 04Mar04. End Date: 19Nov04, Days in Testing = 260

		05Mar04	19Oct04
102–PR&CPP	N06022 ASW PCA KE0137	-148	-93
103	N06022 ASW PCA KE0138	-147	-88
104	N06022 ASW PCA KE0139	-143	-70
105	N06022 ASW PCA KE0140	-148	-96
106–PR&CPP	N06022 ASW + SHT PCA KE0202	-225	101
107	N06022 ASW + SHT PCA KE0203	-244	105
108	N06022 ASW + SHT PCA KE0204	-227	85
109	N06022 ASW + SHT PCA KE0205	-221	18
101	Wrought Platinum Rod WEA016	-214	211

CELL 27: 1 m NaCl + 0.05 m KNO_3 pH 6.67, 100°C [Cl^-/NO_3^- = 20, NO_3^-/Cl^- = 0.05]
Starting Date: 10Mar04. End Date: 19Nov04, Days in Testing = 254

		11Mar04	19Oct04
202–PR&CPP	N06022 ASW PCA KE0141	-174	-88
203	N06022 ASW PCA KE0142	-163	-74
204	N06022 ASW PCA KE0143	-171	-69
205	N06022 ASW PCA KE0144	-163	-92
206–PR&CPP	N06022 ASW + SHT PCA KE0206	-233	23
207	N06022 ASW + SHT PCA KE0207	-196	-26
208	N06022 ASW + SHT PCA KE0208	-184	160
209	N06022 ASW + SHT PCA KE0209	-216	-56
201	Wrought Platinum Rod WEA009	208	243

For all the specimens the Ecorr vs. time was monitored. For the specimens marked PR&CPP the polarization resistance (PR) was regularly monitored and at the end of the immersion time period a cyclic potentiodynamic polarization (CPP) was performed. PCA = Prism Crevice Assembly, ASW = As-Welded. All specimens had a finish of 600-grit paper except the Solution Heat Treated (SHT) (1120°C for 20 min), which had the black annealed (BA) + water quenched (WQ) oxide film on the surface.

TABLE 4
AVERAGE CORROSION RATES (μm/year) FOR INDIVIDUAL SPECIMENS
FOR IMMERSION TIMES HIGHER THAN 250 DAYS

Cell	$[Cl^-]$ (m)	$[NO_3^-]$ (m)	$[Cl]/[NO_3^-]$	CR ASW	SD CR ASW	CR ASW + SHT	SD CR ASW + SHT
26	1	0.15	6.67	0.02296	0.00049	0.05314	0.02394
27	1	0.05	20	0.02430	0.00150	0.02480	0.01405
24	3.5	0.525	6.67	0.02396	0.01149	0.05246	0.02858
25	3.5	0.175	20	0.03119	0.01747	0.01693	0.00433
23	6	0.9	6.67	0.02408	0.00584	0.02030	0.00350
22	6	0.3	20	0.02740	0.00591	0.02776	0.00856

CR = Corrosion Rate, SD = Standard Deviation

TABLE 5
CHARACTERISTIC POTENTIALS FROM CYCLIC POLARIZATION CURVES IN mV, SSC
ASW PCA SPECIMENS AFTER MORE THAN 8 MONTHS IN
NaCl + KNO_3 AERATED ELECTROLYTES AT 100°C

Cell	Specimen	$[Cl^-]$ (m)	$[NO_3^-]$ (m)	$[NO_3^-]/[Cl^-]$	E_{corr}	E20	E200	ER10	ER1	ERCO
26	KE0137 ASW	1	0.15	0.15	-70	577	711	513	410	314
26	KE0202 SHT	1	0.15	0.15	-21	815	971	613	2	NA
27	KE0141 ASW	1	0.05	0.05	-58	581	715	481	30	-32
27	KE0206 SHT	1	0.05	0.05	143	751	962	162	NA (<143)	NA
24	KE0129 ASW	3.5	0.525	0.15	-148	611	788	526	380	273
24	KE0194 SHT	3.5	0.525	0.15	-32	822	937	98	-1	NA
25	KE0133 ASW	3.5	0.175	0.05	-127	597	752	533	7	-61
25	KE0198 SHT	3.5	0.175	0.05	-8	702	922	NA	NA (<-8)	NA
23	KE0125 ASW	6	0.9	0.15	-75	726	873	637	382	46
23	KE0190 SHT	6	0.9	0.15	140	678	867	572	NA (<139)	NA
22	KE0124 ASW	6	0.3	0.05	-119	676	826	586	-10	-37
22	KE0189 SHT	6	0.3	0.05	16	565	884	24	NA (<16)	NA

E_{corr} is the corrosion potential before the CPP was started. NA = Not available because the test ended before these values of current density were reached.

TABLE 6
CHARACTERISTIC POTENTIALS FROM POLARIZATION CURVES IN mV, SSC
FRESHLY POLISHED SPECIMENS AFTER 24-h IMMERSION IN
$NaCl + KNO_3$ DEAERATED ELECTROLYTES AT 100°C

Specimen	$[Cl^-]$ (m)	$[NO_3^-]$ (m)	$[NO_3^-]/[Cl^-]$	E_{corr}	E20	E200	ER10	ER1	ERCO
JE3220 ASW MCA	1	0.15	0.15	-497	NA	NA	590	21	15
JE3237 ASW MCA	1	0.15	0.15	-513	402	NA	148	-50	-65
JE3225 ASW MCA	1	0.05	0.05	-526	443	NA	-18	-104	-119
JE3236 ASW MCA	1	0.05	0.05	-505	404	NA	-43	-116	-122
KE0356 ASW PCA	1	0.05	0.05	-684	368	700	-19	-82	-86
KE0360 ASW PCA	1	0.05	0.05	-643	317	516	-14	-78	-81
KE0361 ASW PCA	1	0.05	0.05	-629	345	723	1	-62	-64
DEA3385 MA MCA	3.5	0.525	0.15	-340	448	NA	80	-74	-82
DEA3386 MA MCA	3.5	0.525	0.15	-207	337	NA	177	-8	111
DEA3390 MA MCA	3.5	0.525	0.15	-480	425	682	333	-5	-81
JE1773 ASW MCA	3.5	0.525	0.15	-524	385	697	78	-68	-85
JE3242 ASW MCA	3.5	0.525	0.15	-285	375	NA	264	-62	-96
JE3221 ASW MCA	3.5	0.175	0.05	-553	390	NA	-40	-119	-132
JE3239 ASW MCA	3.5	0.175	0.05	-411	390	557	-50	-101	-104
JE3319 MA MCA	6	0.9	0.15	-460	430	737	-6	-77	-84
JE3320 MA MCA	6	0.9	0.15	-486	527	777	-8	-82	-88
KE0415 ASW PCA	6	0.9	0.15	-516	485	757	17	-73	-77
KE0416 ASW PCA	6	0.9	0.15	-528	545	792	500	-62	-77
KE0417 ASW PCA	6	0.9	0.15	-528	597	791	605	-31	-59
JE3215 ASW MCA	6	0.9	0.15	-505	442	NA	18	-75	-85
JE3240 ASW MCA	6	0.9	0.15	-340	425	NA	356	-22	-40
JE3315 MA MCA	6	0.3	0.05	-259	278	402	-47	-84	-88
JE3316 MA MCA	6	0.3	0.05	-533	211	315	-53	-78	-79
JE3201 ASW MCA	6	0.3	0.05	-531	288	402	-47	-85	-88
JE3223 ASW MCA	6	0.3	0.05	-507	240	330	-56	-114	-120
KE0358 ASW PCA	6	0.3	0.05	-601	277	418	-41	-88	-93
KE0359 ASW PCA	6	0.3	0.05	-592	264	384	-18	-58	-61

TABLE 7
OBSERVATION FROM SPECIMENS EXPOSED >8 MONTHS IN AERATED ELECTROLYTES AT 100°c

Cell	Specimens	$[Cl^-]$ (m)	$[NO_3^-]$ (m)	Observations
23	ASW KE0126-128	6	0.9	Specimens light metallic blue. No GC. One small spot CC per specimen (KE0126 = none)
23	ASW + SHT KE0191-193	6	0.9	Specimens dark green black, iridescent. No GC. CC in one to three spots where the PTFE tape was adhered to the specimen.
22	ASW KE0121-123	6	0.3	Specimens bluish/golden in area outside CF. No GC no CC.
22	ASW + SHT KE0186-188	6	0.3	Specimens dark green, gray and black. Also iridescent colors. CC in several spots in each specimen
24	ASW KE0130-132	3.5	0.525	Specimens blue, yellow, iridescent. No GC. No CC.
24	ASW + SHT KE0195-197	3.5	0.525	Specimens dark green with blue-brown halos. No GC. No CC.
25	ASW KE0134-136	3.5	0.175	Slight discoloration, some iridescent-golden-blue halos. No GC. No CC.
25	ASW + SHT KE0199-201	3.5	0.175	Dark gray-green. Blue-brown halos. Minimal CC. No GC.
26	ASW KE0138-140	1	0.15	Shiny bluish-yellowish. Some halos. No CC. No GC.
26	ASW + SHT KE0203-205	1	0.15	Dark gray-green. Halos of blue-yellow. 1 spot of CC (KE0204).
27	ASW KE0142-144	1	0.05	Little discoloration. Gray-golden-iridescent. No CC. No GC.
27	ASW + SHT KE0207-209	1	0.05	Dark gray-green-iridescent. Small CC (few spots). No GC.

GC = General Corrosion, CC = Crevice Corrosion, PTFE = polytetrafluoroethylene, CF = Crevice Formers

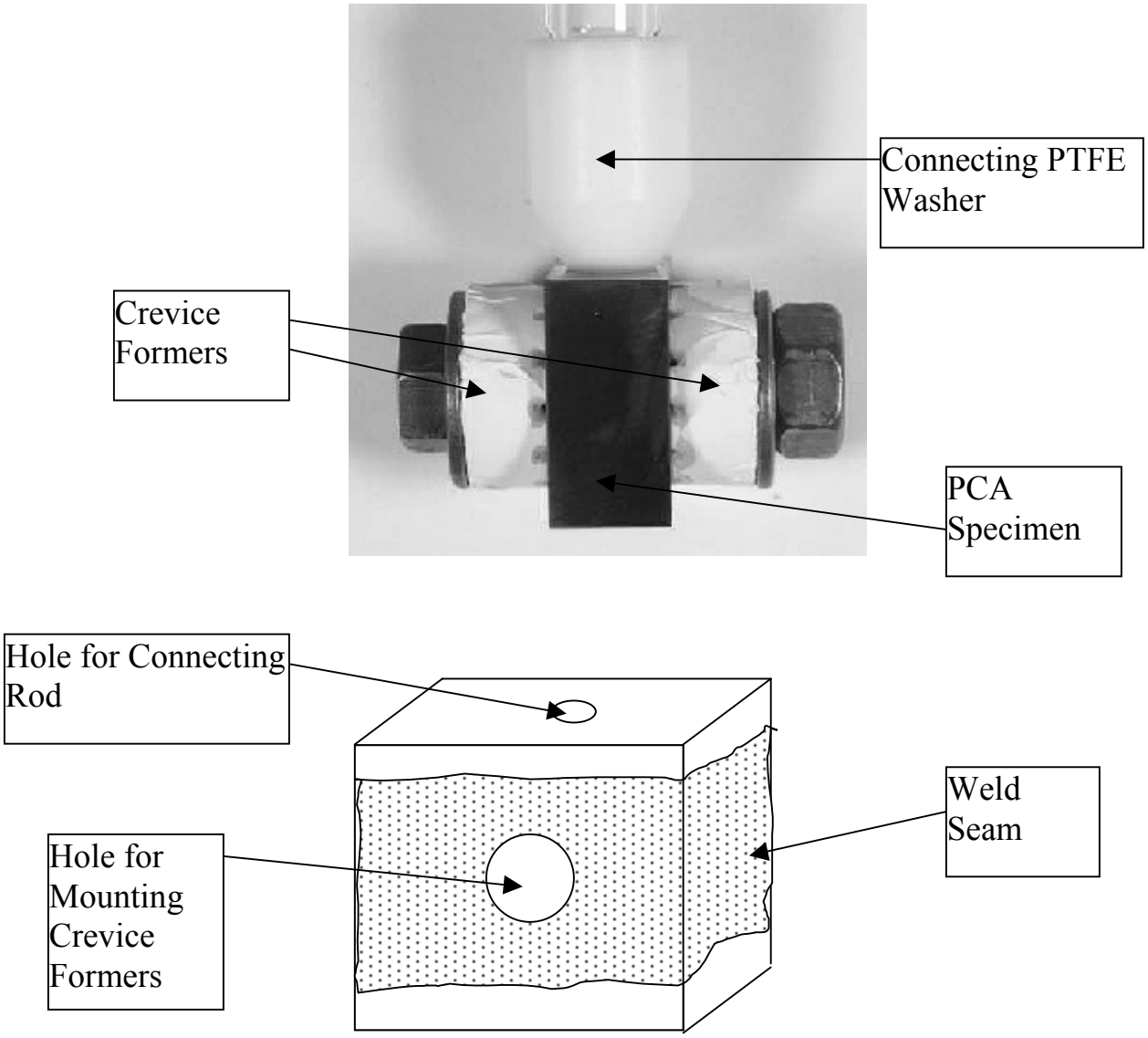

FIGURE 1 - PCA Specimen (0.75 x 0.75 x 0.375 inch or approx. 20 x 20 x 10 mm), The weld seam was not the same width on both faces of the specimen.

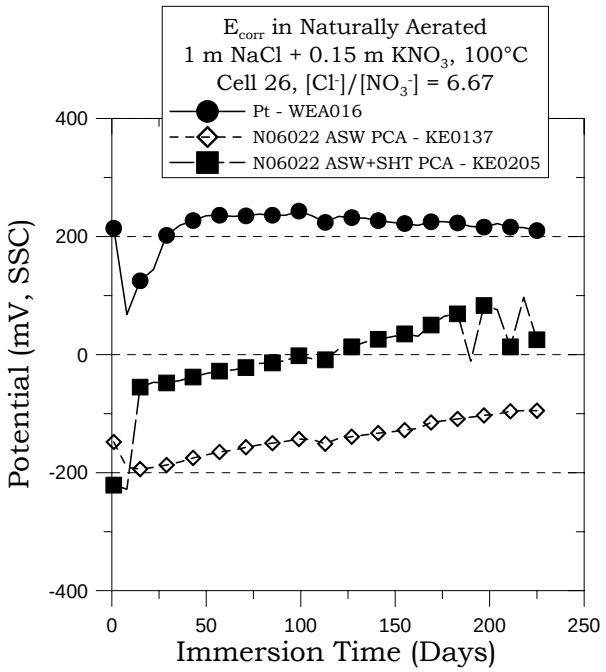

FIGURE 2 – E_{corr} vs. Time Cell 26

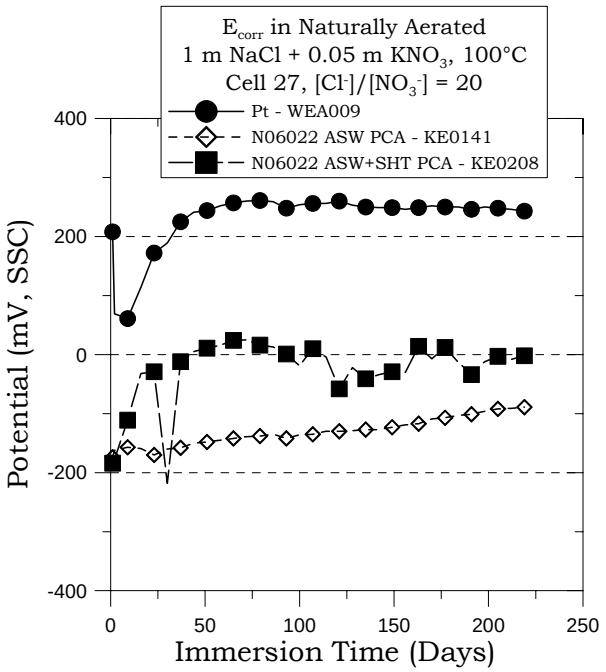

FIGURE 3 – E_{corr} vs. Time Cell 27

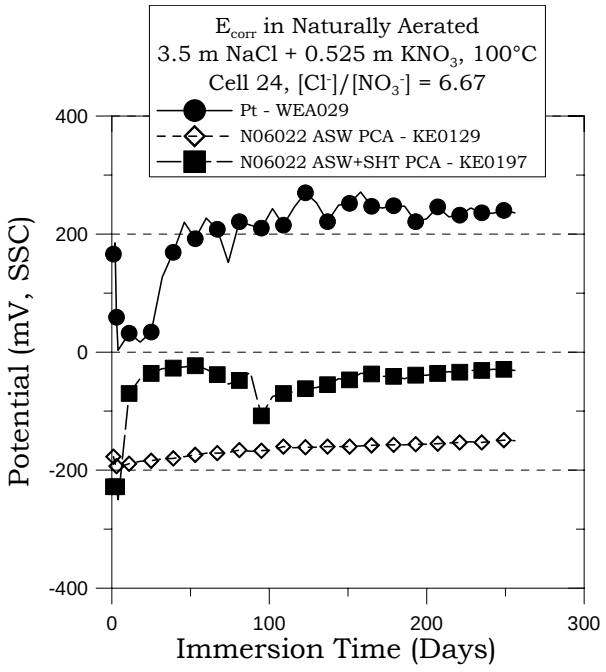

FIGURE 4 – E_{corr} vs. Time Cell 24

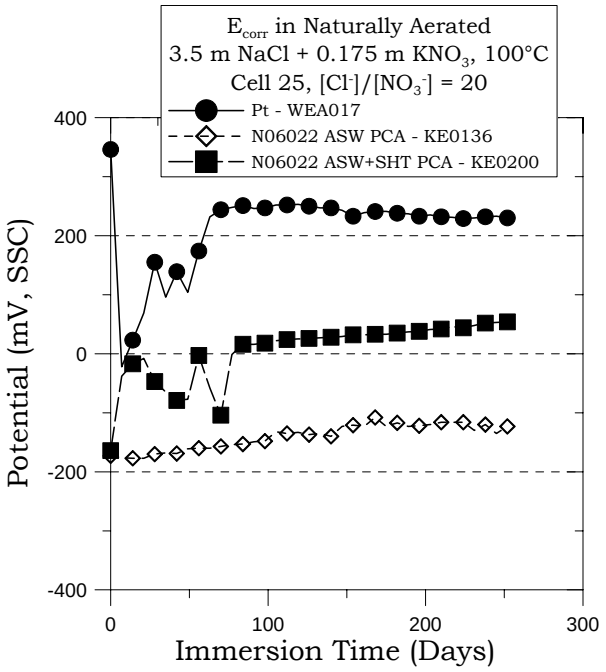

FIGURE 5 – E_{corr} vs. Time Cell 25

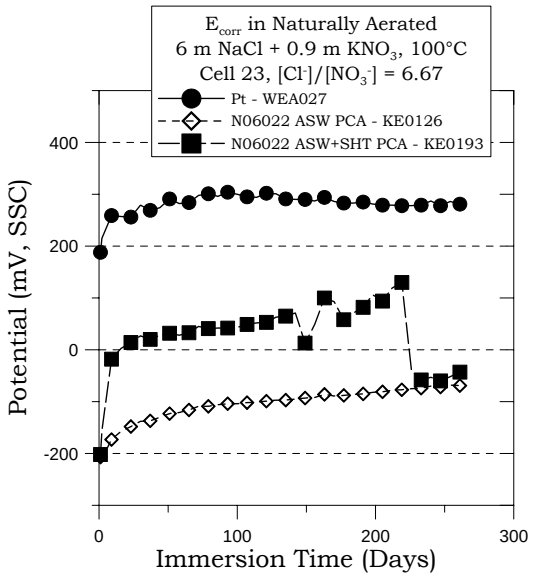

FIGURE 6 – E_{corr} vs. Time Cell 23

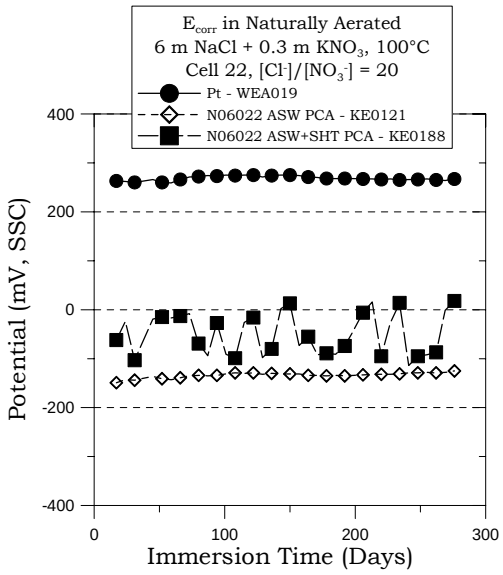

FIGURE 7 – E_{corr} vs. Time Cell 22

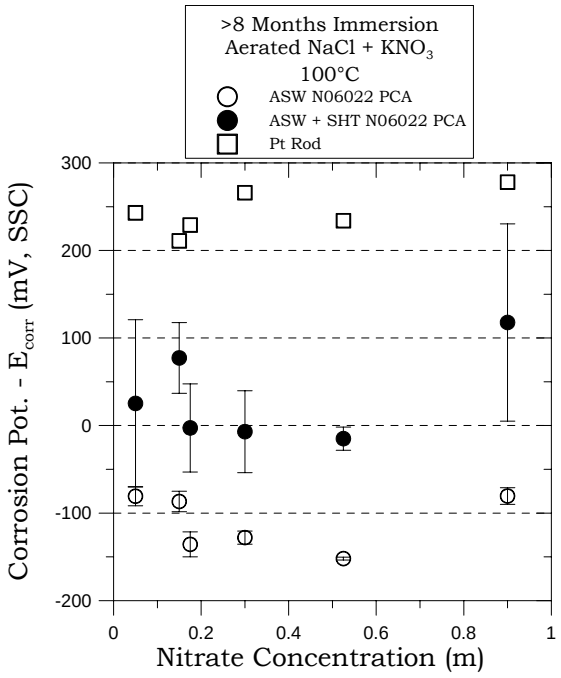

FIGURE 8 – E_{corr} >8 Months vs. Nitrate Concentration for all Cells

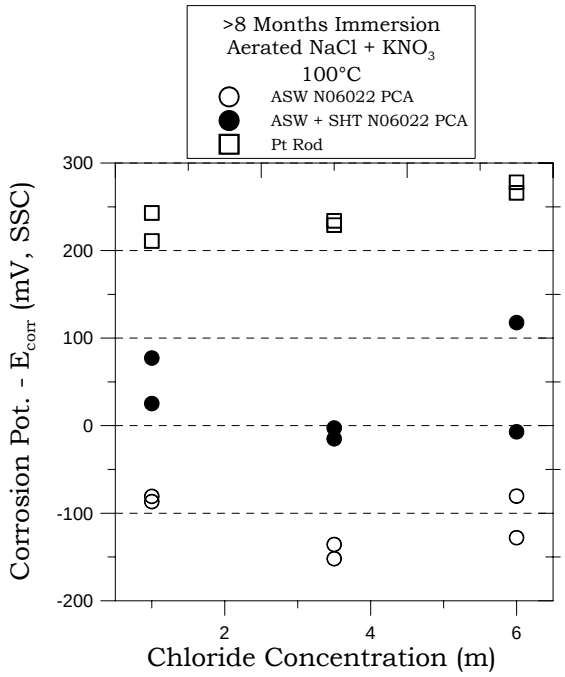

FIGURE 9 – E_{corr} >8 Months vs. Chloride Concentration for all Cells

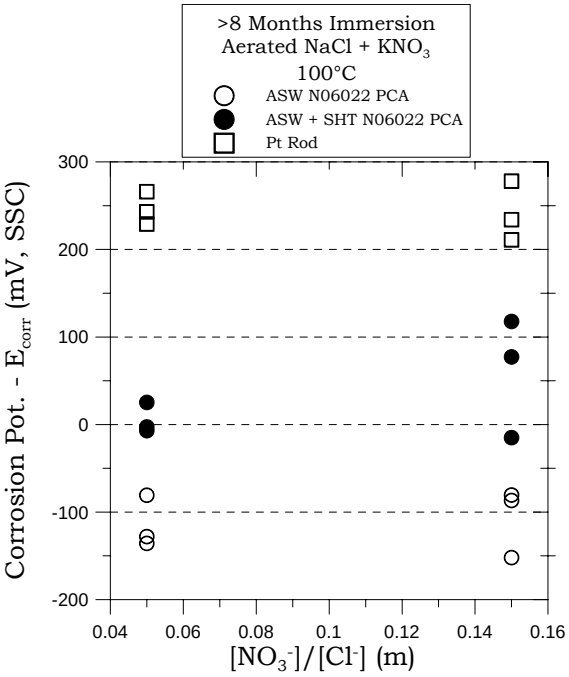

FIGURE 10 – E_{corr} >8 Months vs. Nitrate/Chloride Concentration for all Cells

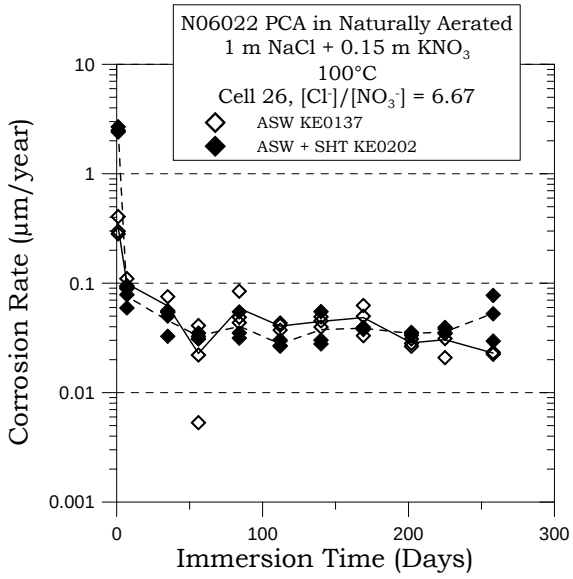

FIGURE 11 – Corrosion Rate vs. Time Cell 26

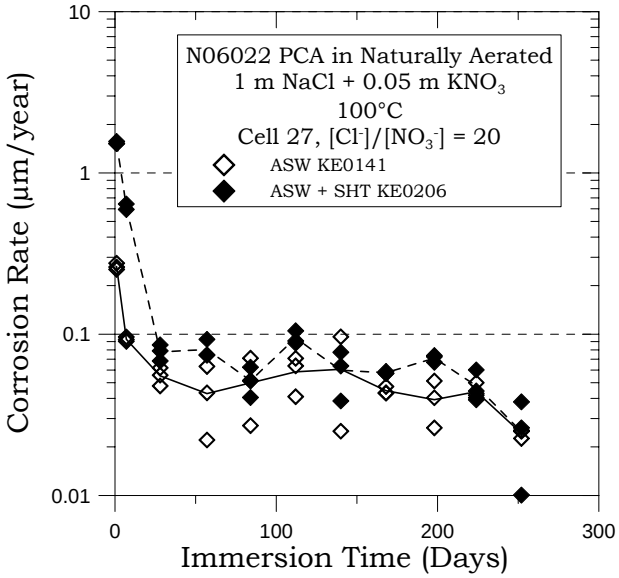

FIGURE 12 – Corrosion Rate vs. Time Cell 27

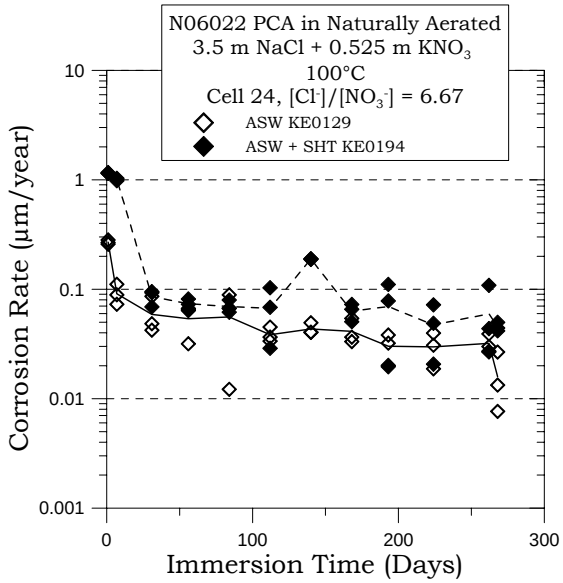

FIGURE 13 – Corrosion Rate vs. Time Cell 24

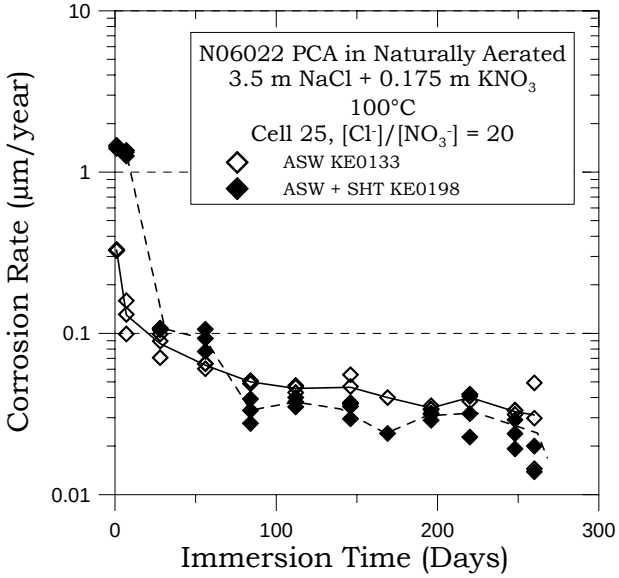

FIGURE 14 – Corrosion Rate vs. Time Cell 25

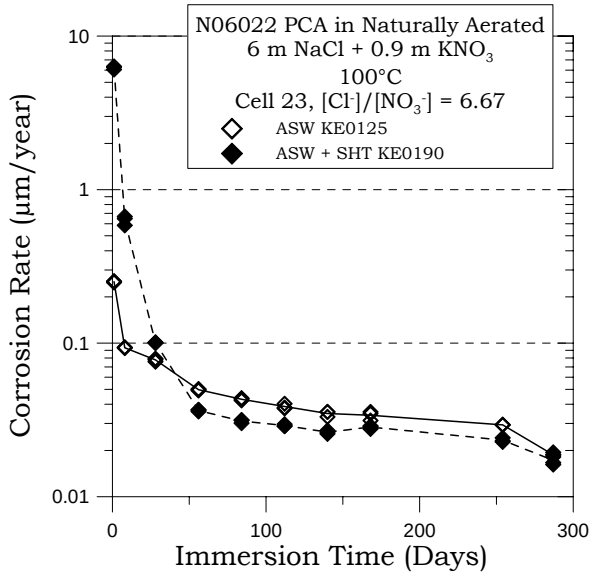

FIGURE 15 – Corrosion Rate vs. Time Cell 23

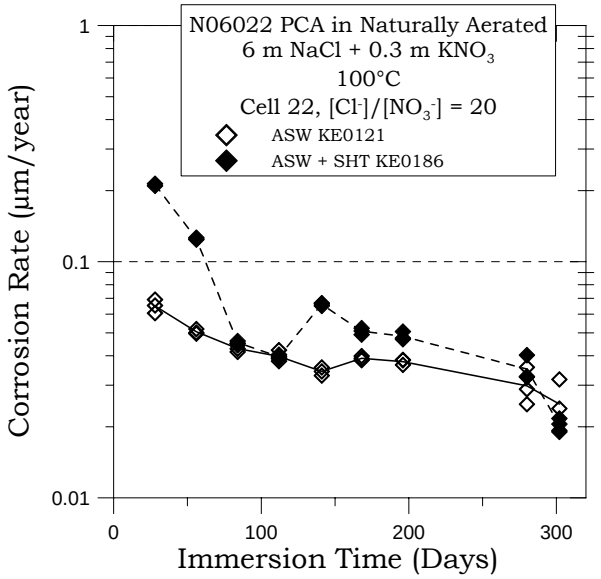

FIGURE 16 – Corrosion Rate vs. Time Cell 22

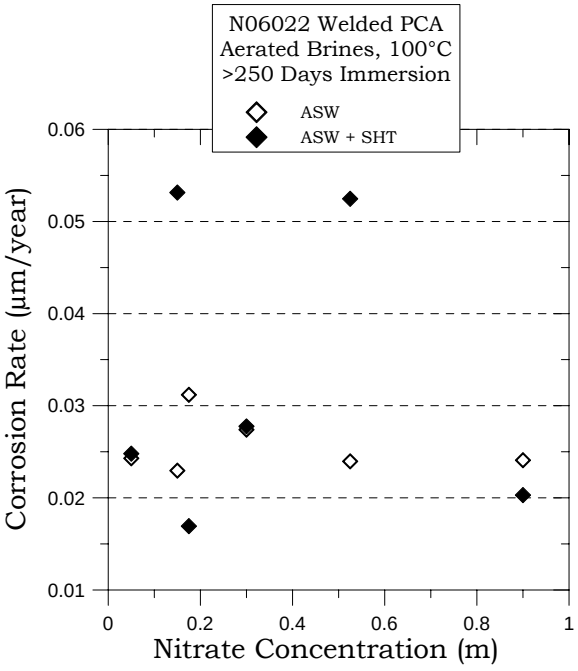

FIGURE 17 – Corrosion Rate vs. Nitrate Concentration (Cells 22-27)

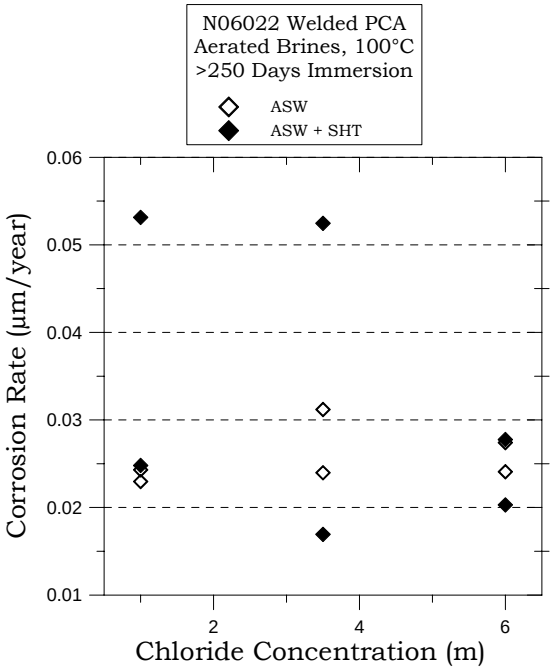

FIGURE 18 – Corrosion Rate vs. Chloride Concentration (Cells 22-27)

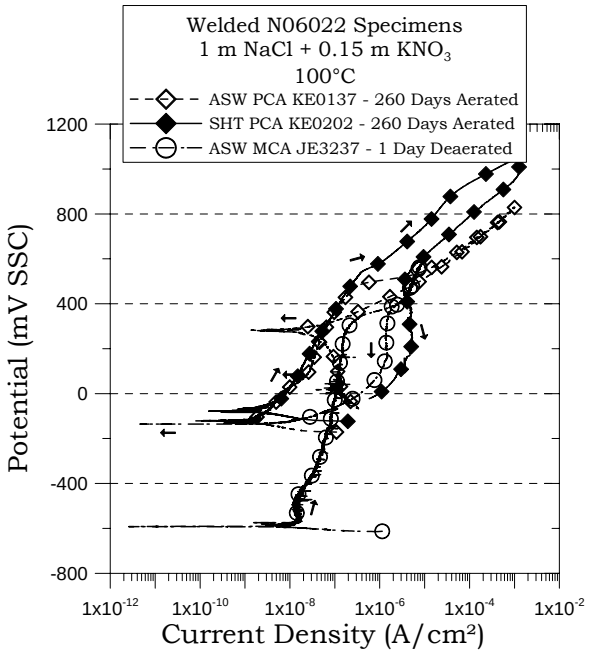

FIGURE 19 – Polarization Curves (CPP) Cell 26

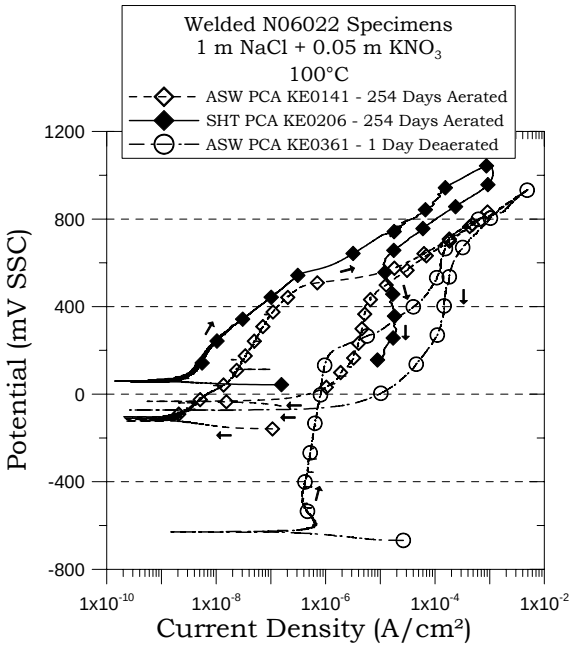

FIGURE 20 – Polarization Curves (CPP) Cell 27

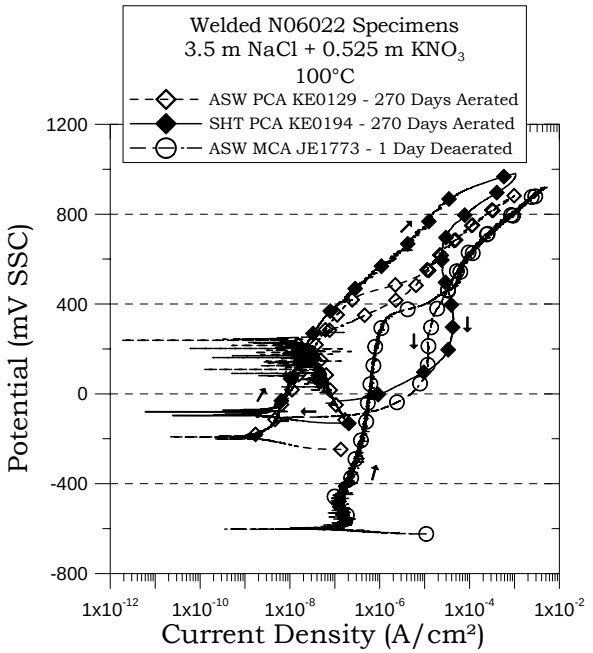

FIGURE 21 – Polarization Curves (CPP) Cell 24

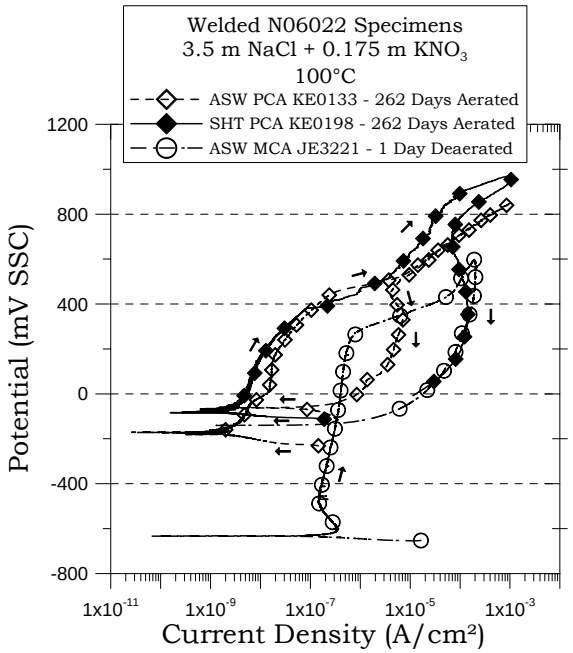

FIGURE 22 – Polarization Curves (CPP) Cell 25

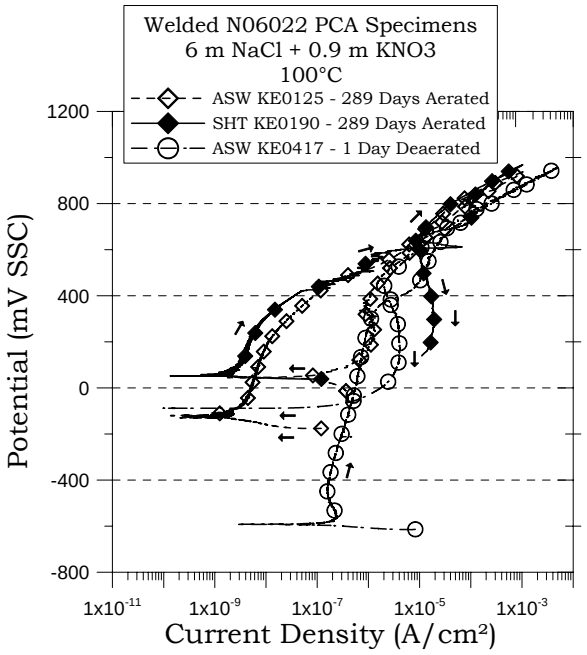

FIGURE 23 – Polarization Curves (CPP) Cell 23

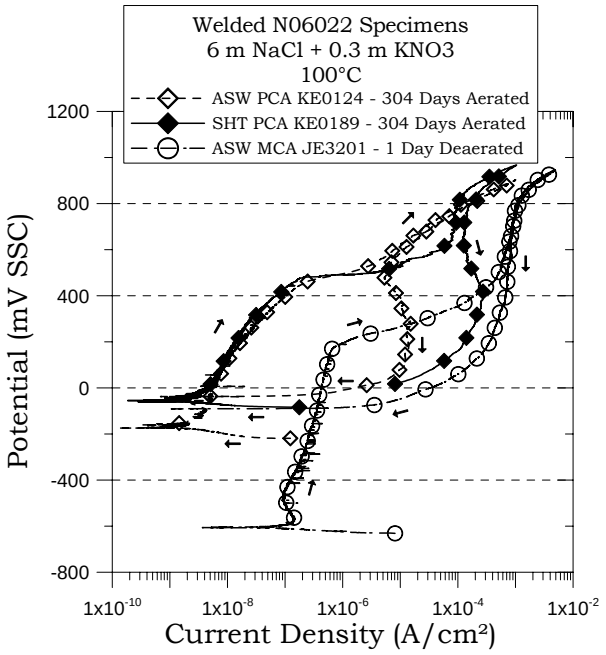

FIGURE 24 – Polarization Curves (CPP) Cell 22

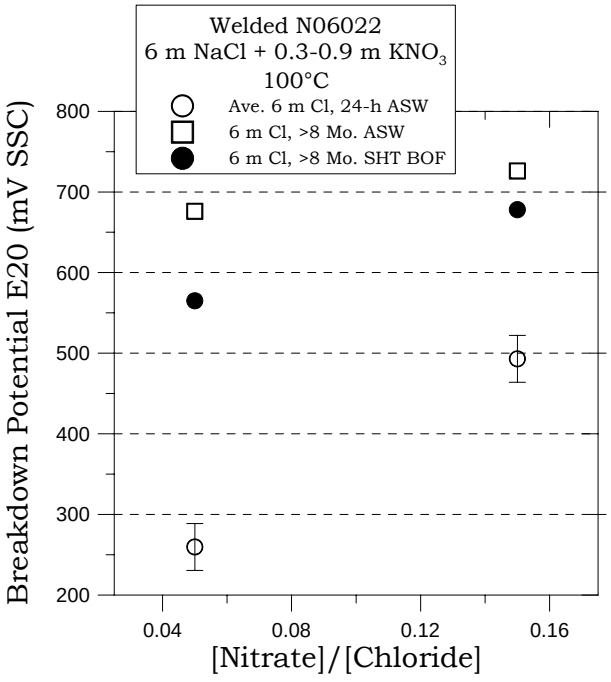

FIGURE 25 – Breakdown Potential (E20) Comparing Effect of Immersion Time for a 6 m NaCl solution at 100°C.

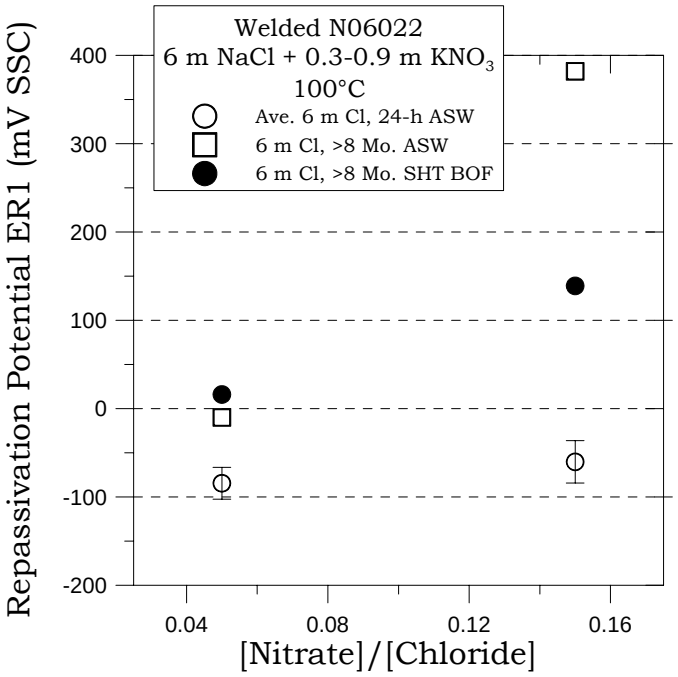

FIGURE 26 – Repassivation Potential (ER1) Comparing Effect of Immersion Time.

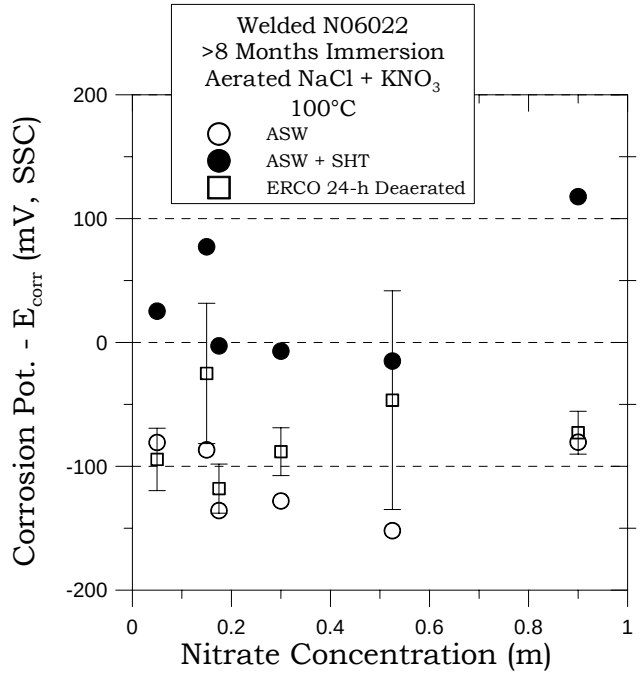

FIGURE 27 – >8 Months E_{corr} compared to ERCO for ASW and ASW + SHT specimens